Supporting Information

# Efficient ketose production by hydroxyapatite catalyst in a continuous flow module

Kaho Usami, Kejing Xiao, and Akimitsu Okamoto*

**Table of Contents**

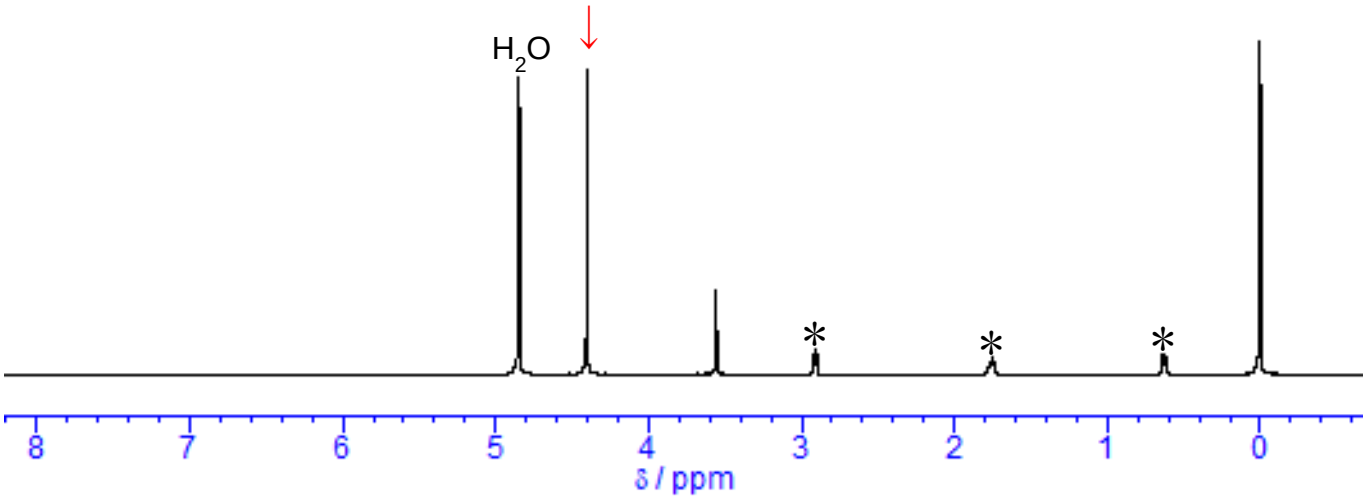


**Figure S1.** A full-range $^{1}$H-NMR chart of dihydroxyacetone in $D_2O$. The peaks indicated by * and a peak at 0 ppm are derived from an internal standard 4,4-dimethyl-4-silapentane-1-sulfonic acid. A red arrow indicates a standard peak used for the calculation of the conversion yield.

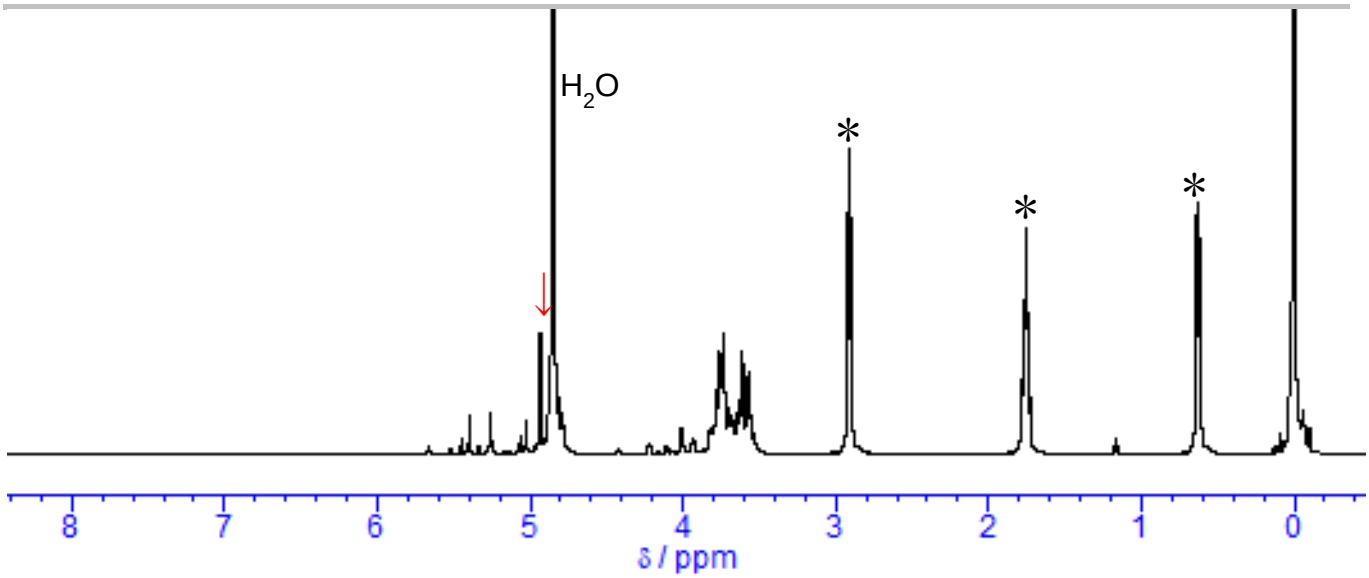


**Figure S2.** A full-range $^{1}$H-NMR chart of $_{DL}$-glyceraldehyde in $D_2O$. The peaks indicated by * and a peak at 0 ppm are derived from an internal standard 4,4-dimethyl-4-silapentane-1-sulfonic acid. A red arrow indicates a standard peak used for the calculation of the conversion yield.

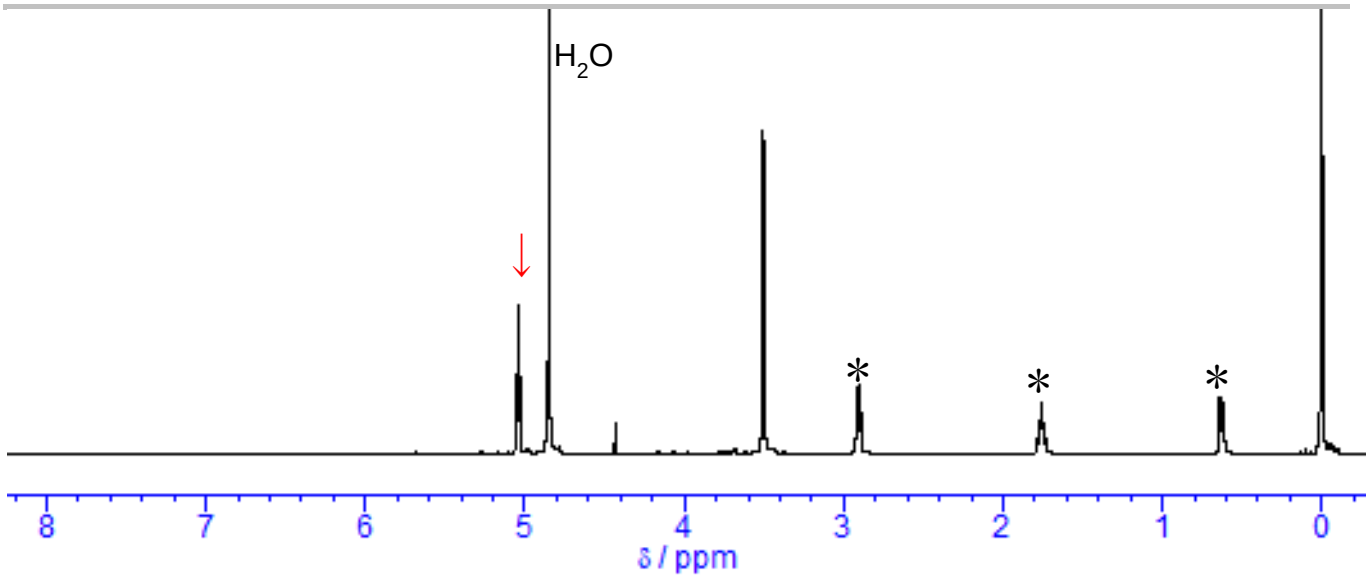


**Figure S3.** A full-range $^{1}$H-NMR chart of glycolaldehyde in $D_2O$. The peaks indicated by * and a peak at 0 ppm are derived from an internal standard 4,4-dimethyl-4-silapentane-1-sulfonic acid. A red arrow indicates a standard peak used for the calculation of the conversion yield.

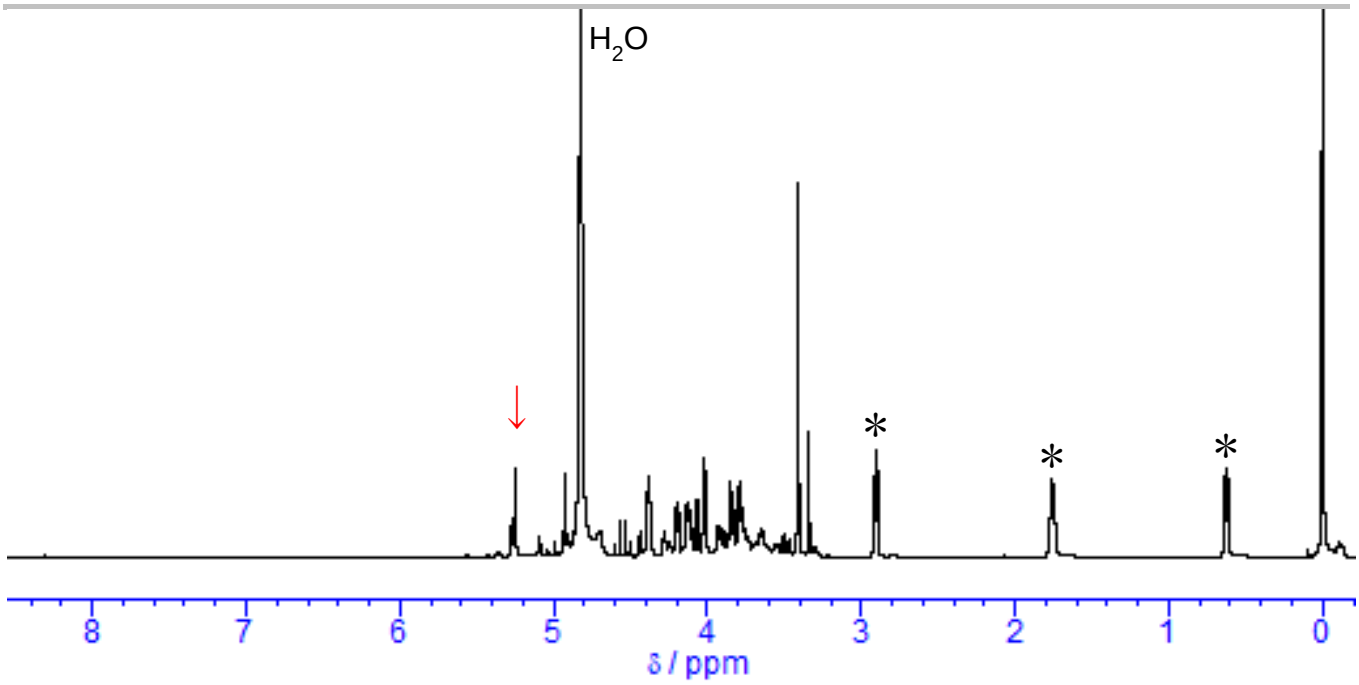


**Figure S4.** A full-range $^{1}$H-NMR chart of erythrose in $D_2O$. The peaks indicated by * and a peak at 0 ppm are derived from an internal standard 4,4-dimethyl-4-silapentane-1-sulfonic acid. A red arrow indicates a standard peak used for the calculation of the conversion yield.

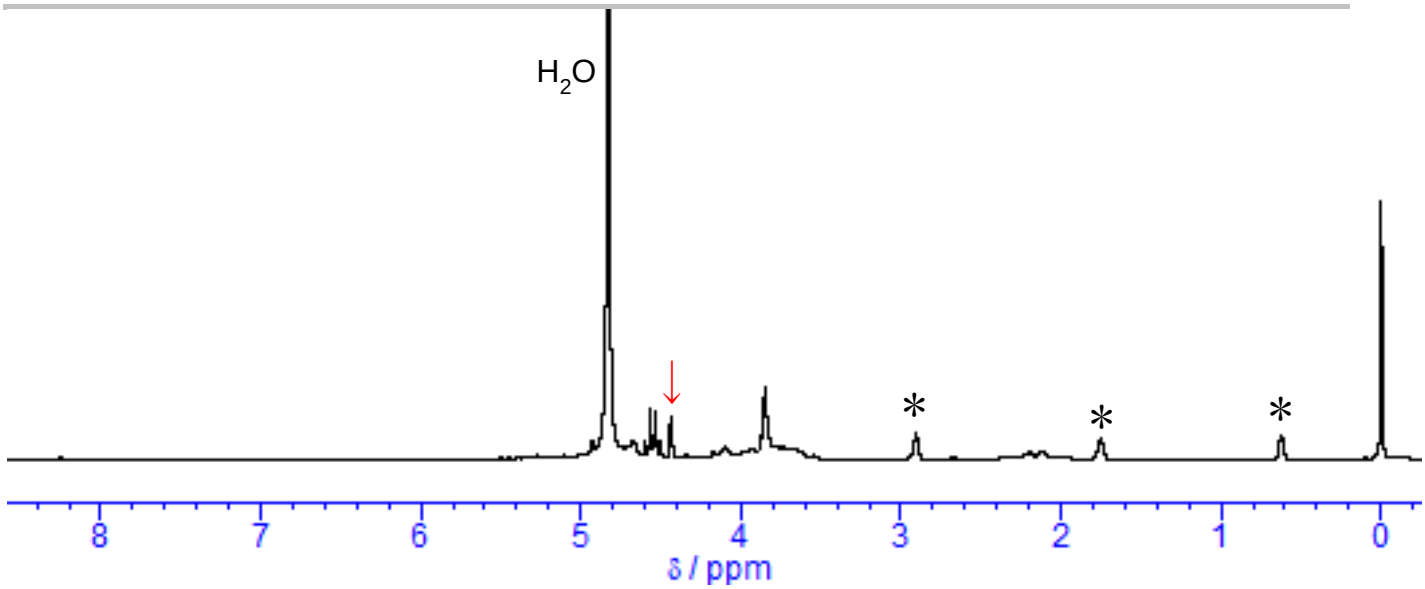


**Figure S5.** A full-range $^{1}$H-NMR chart of erythrulose in $D_2O$. The peaks indicated by * and a peak at 0 ppm are derived from an internal standard 4,4-dimethyl-4-silapentane-1-sulfonic acid. A red arrow indicates a standard peak used for the calculation of the conversion yield.

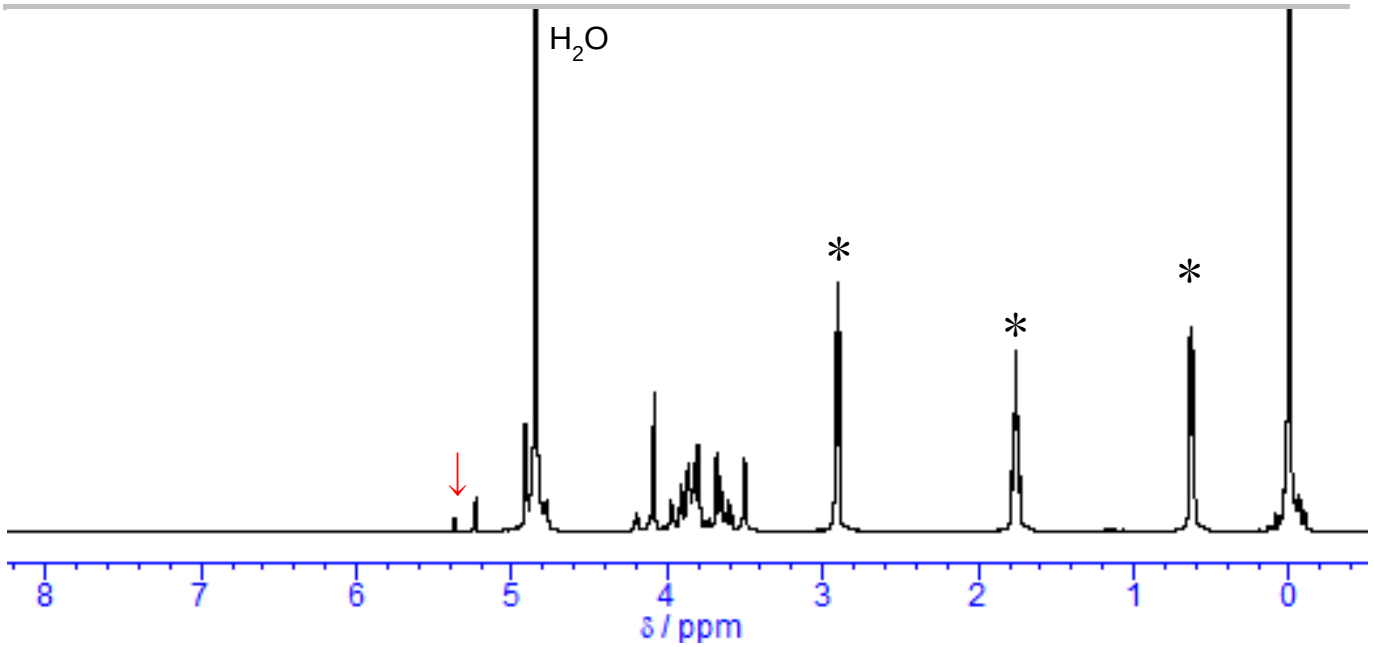


**Figure S6.** A full-range $^{1}$H-NMR chart of ribose in $D_2O$. The peaks indicated by * and a peak at 0 ppm are derived from an internal standard 4,4-dimethyl-4-silapentane-1-sulfonic acid. A red arrow indicates a standard peak used for the calculation of the conversion yield.

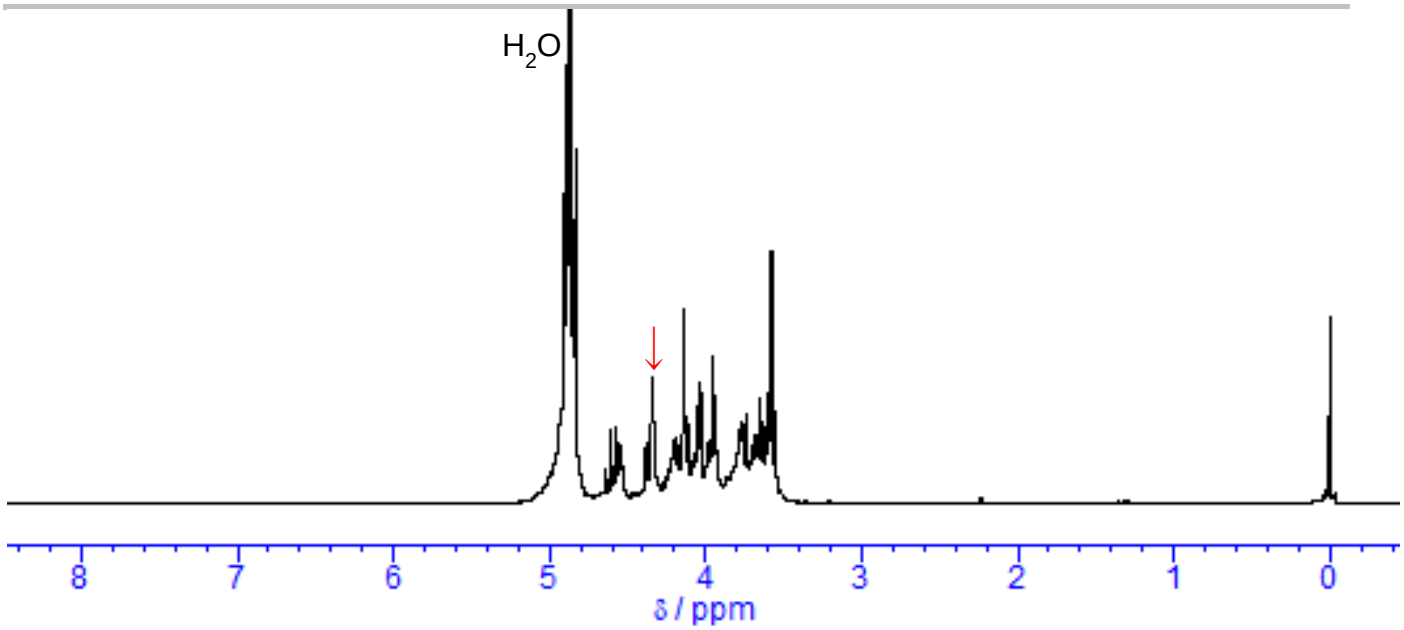


**Figure S7.** A full-range $^{1}$H-NMR chart of ribulose in $D_2O$. A red arrow indicates a standard peak used for the calculation of the conversion yield.

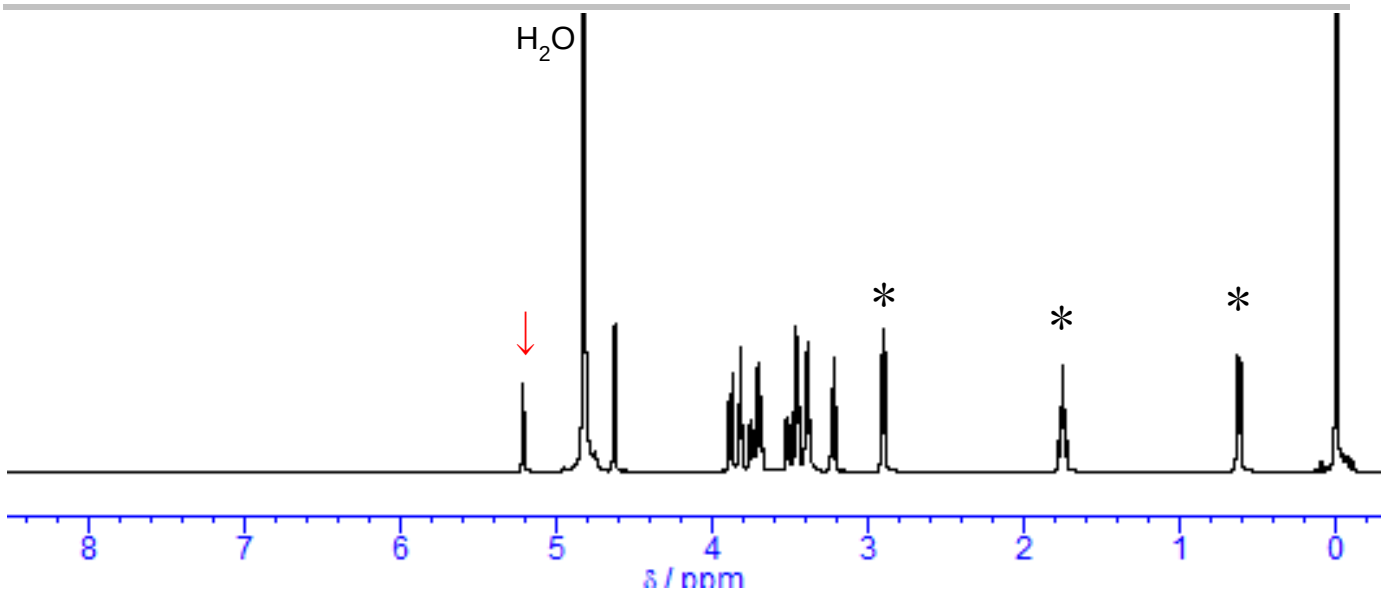


**Figure S8.** A full-range $^{1}$H-NMR chart of glucose in $D_2O$. The peaks indicated by * and a peak at 0 ppm are derived from an internal standard 4,4-dimethyl-4-silapentane-1-sulfonic acid. A red arrow indicates a standard peak used for the calculation of the conversion yield.

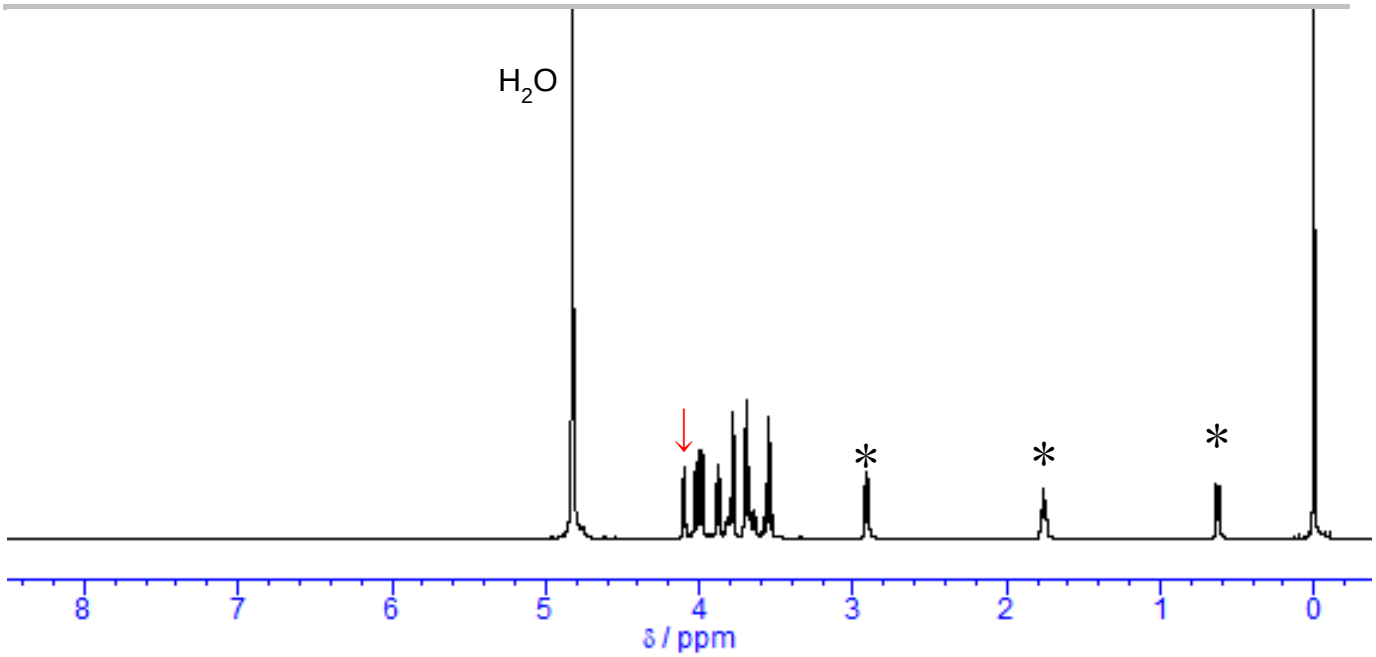


**Figure S9.** A full-range $^{1}$H-NMR chart of fructose in $D_2O$. The peaks indicated by * and a peak at 0 ppm are derived from an internal standard 4,4-dimethyl-4-silapentane-1-sulfonic acid. A red arrow indicates a standard peak used for the calculation of the conversion yield.

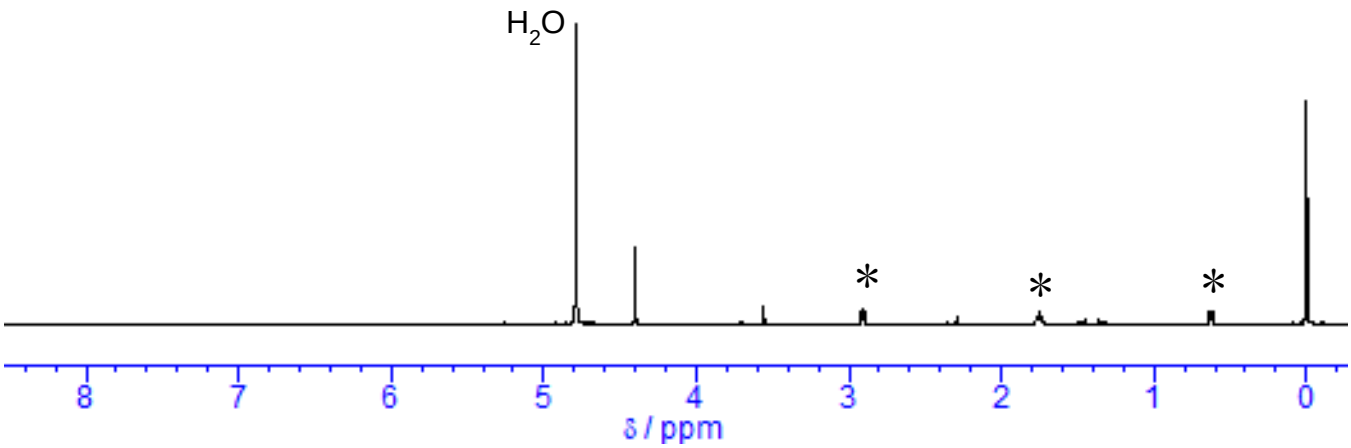


**Figure S10.** A full-range $^{1}$H-NMR chart of the reaction products in entry 5 of Table 1. The peaks indicated by * and a peak at 0 ppm are derived from an internal standard 4,4-dimethyl-4-silapentane-1-sulfonic acid.

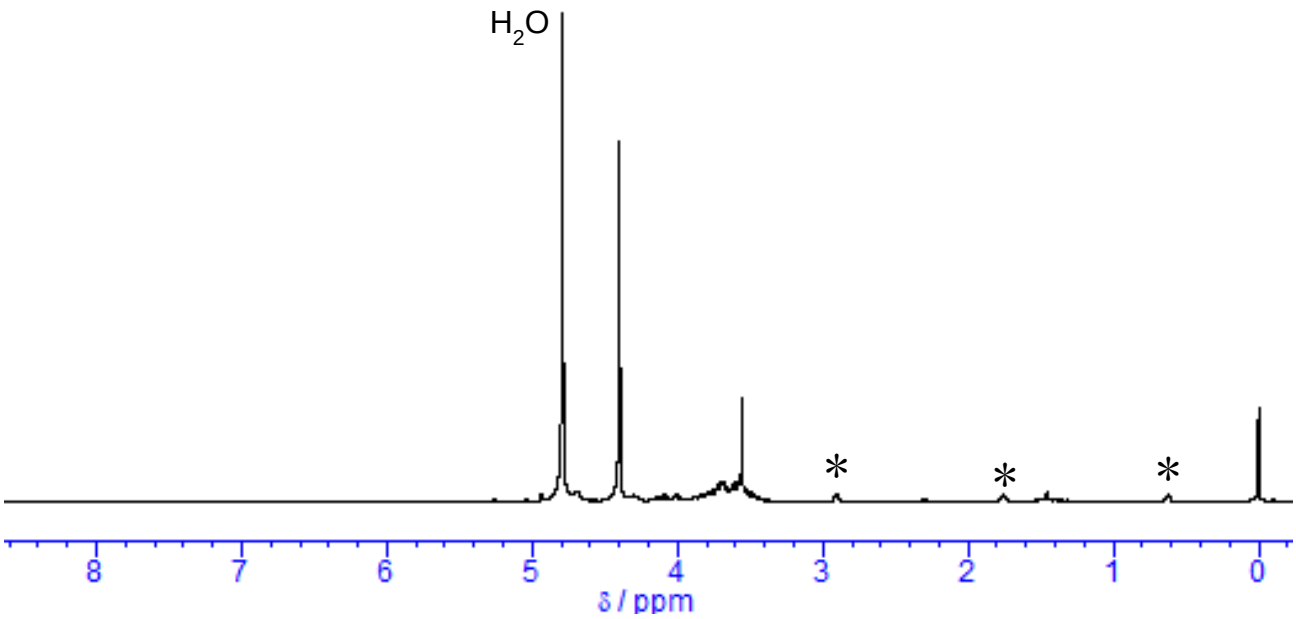


**Figure S11.** A full-range $^{1}$H-NMR chart of the reaction products in entry 3 of Table 1 (entry 1 of Table 2). The peaks indicated by * and a peak at 0 ppm are derived from an internal standard 4,4-dimethyl-4-silapentane-1-sulfonic acid.

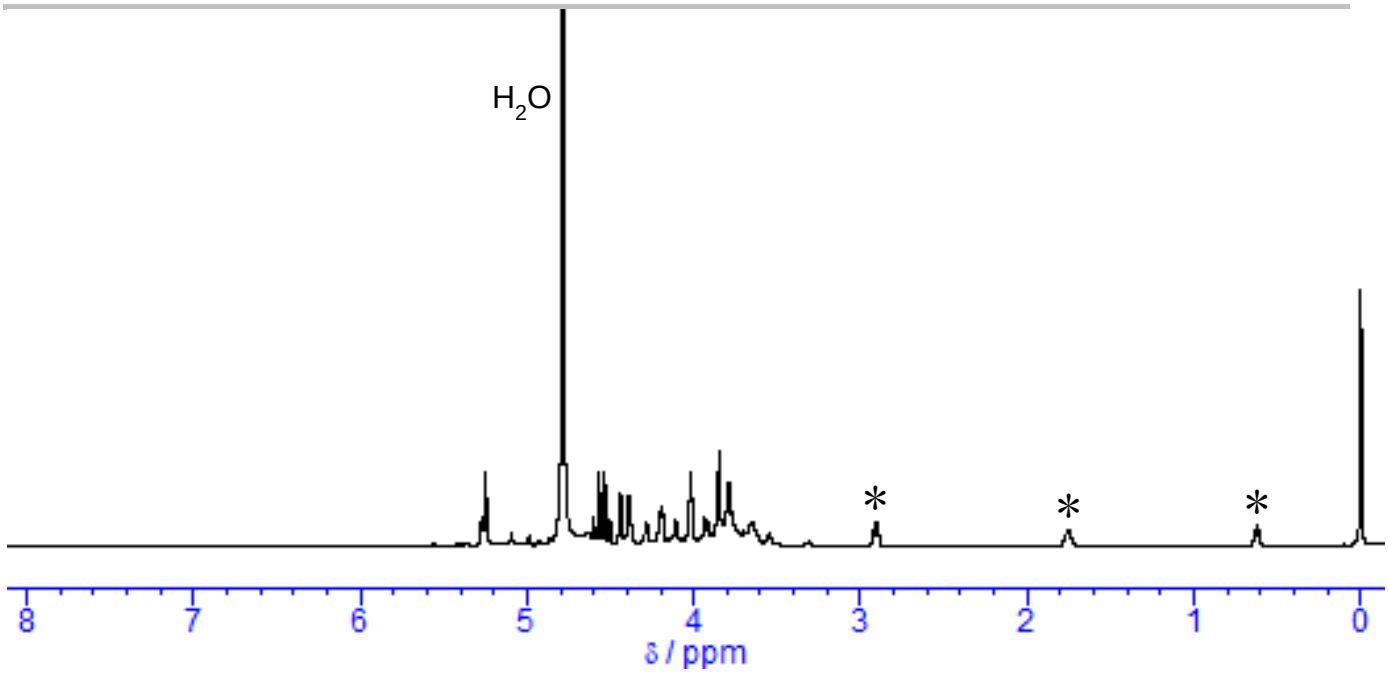


**Figure S12.** A full-range $^{1}$H-NMR chart of the reaction products in entry 2 of Table 2. The peaks indicated by * and a peak at 0 ppm are derived from an internal standard 4,4-dimethyl-4-silapentane-1-sulfonic acid.

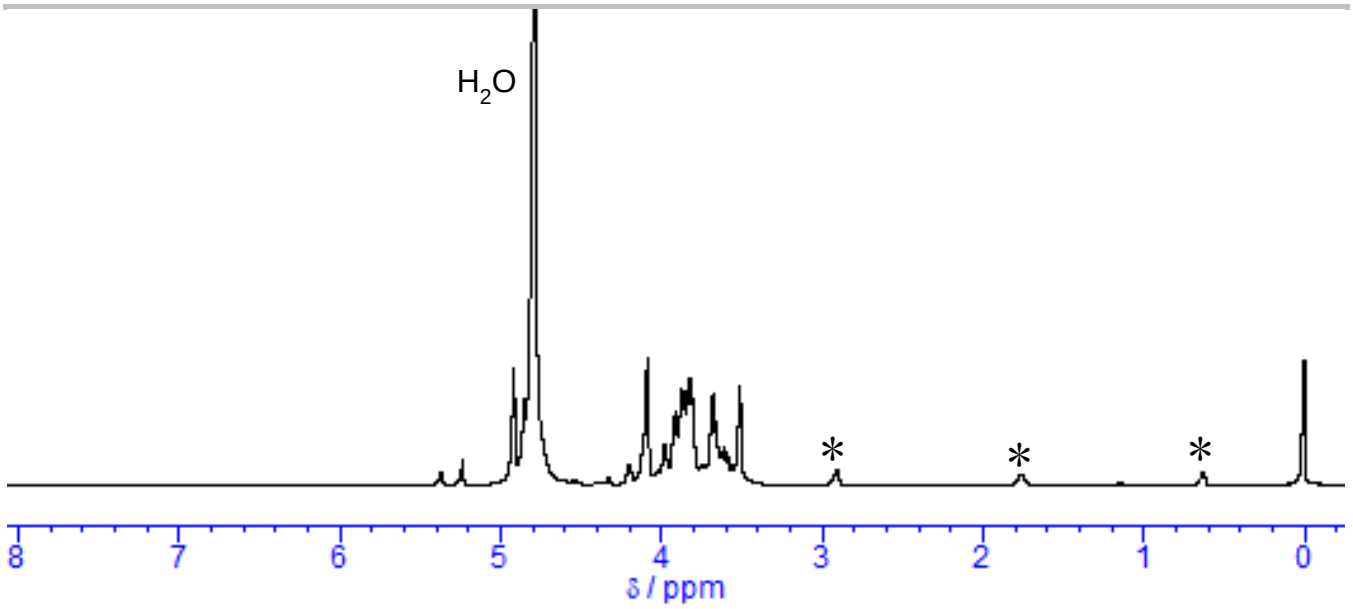


**Figure S13.** A full-range $^{1}$H-NMR chart of the reaction products in entry 3 of Table 2. The peaks indicated by * and a peak at 0 ppm are derived from an internal standard 4,4-dimethyl-4-silapentane-1-sulfonic acid.

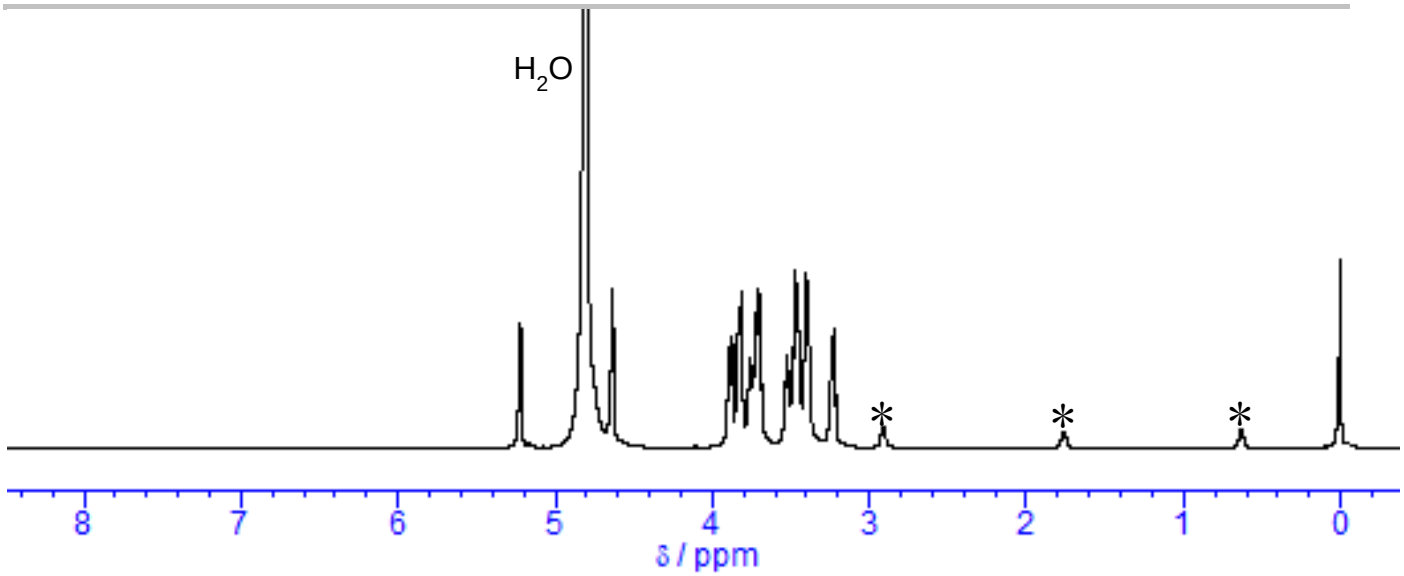


**Figure S14.** A full-range $^{1}$H-NMR chart of the reaction products in entry 4 of Table 2. The peaks indicated by * and a peak at 0 ppm are derived from an internal standard 4,4-dimethyl-4-silapentane-1-sulfonic acid.

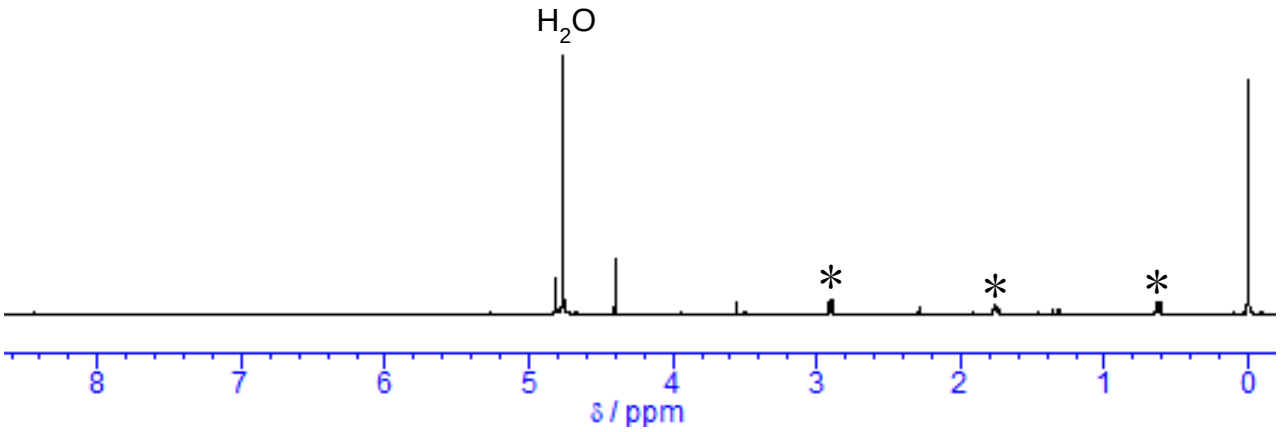


**Figure S15.** A full-range $^{1}$H-NMR chart of the reaction products in entry 4 of Table 3. The peaks indicated by * and a peak at 0 ppm are derived from an internal standard 4,4-dimethyl-4-silapentane-1-sulfonic acid.

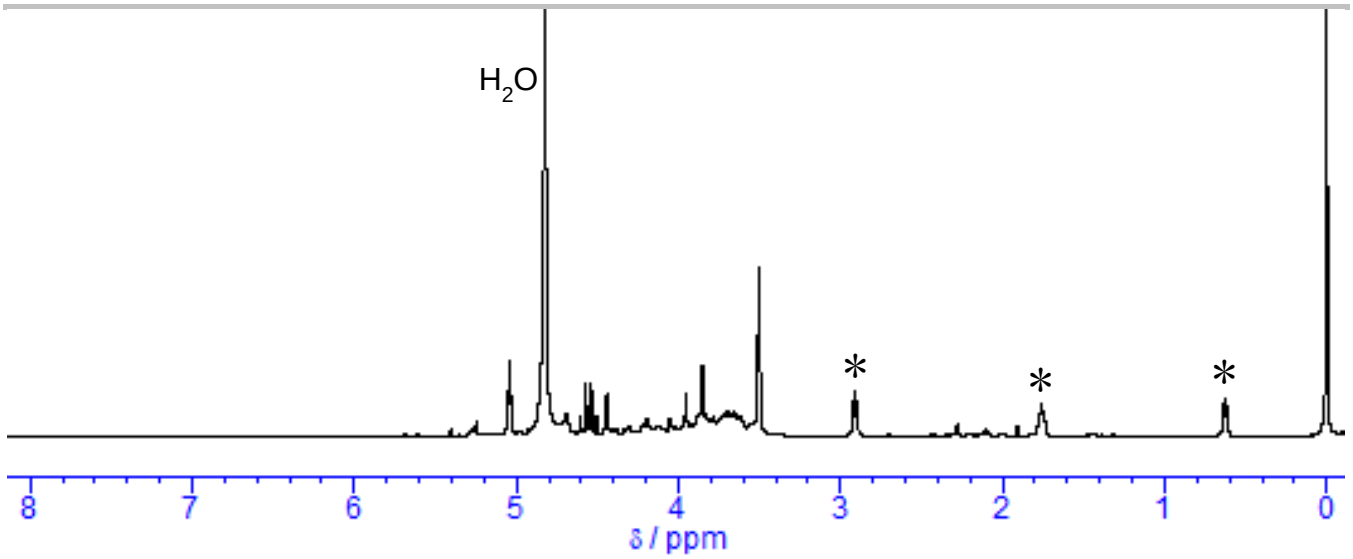


**Figure S16.** A full-range $^{1}$H-NMR chart of the products in the self-aldol reaction of glycolaldehyde. The peaks indicated by * and a peak at 0 ppm are derived from an internal standard 4,4-dimethyl-4-silapentane-1-sulfonic acid.

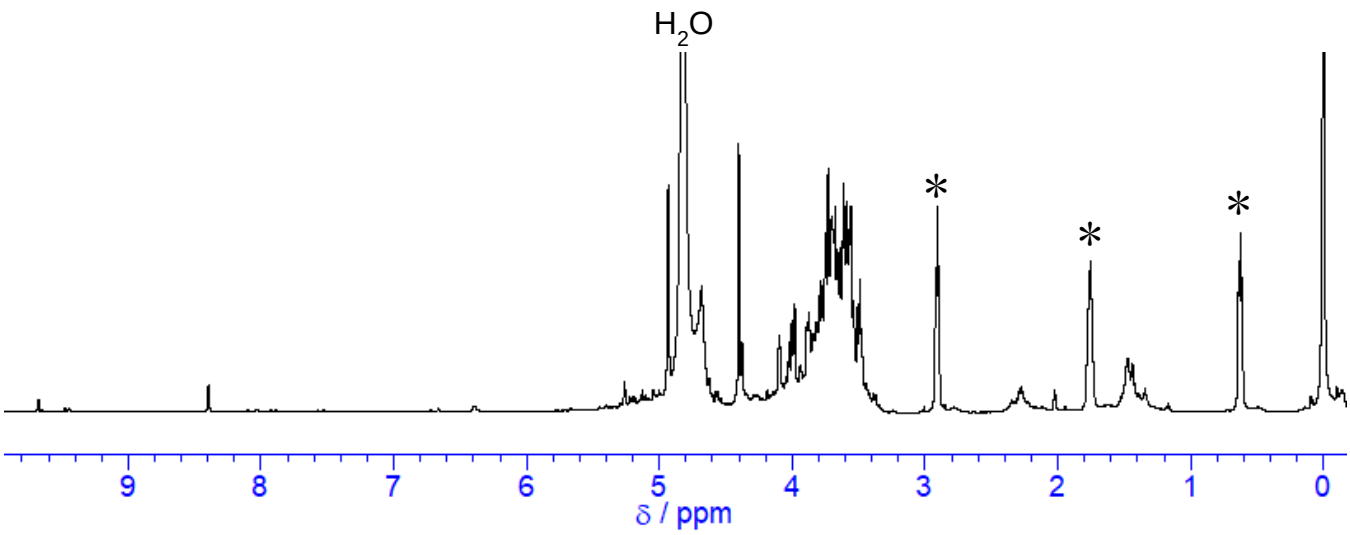


**Figure S17.** A full-range $^{1}$H-NMR chart of the HAp-catalyzed isomerization of glyceraldehyde in $D_2O$. The peaks indicated by * and a peak at 0 ppm are derived from an internal standard 4,4-dimethyl-4-silapentane-1-sulfonic acid.